Available online at www.sciencedirect.com
SCIENCE DIRECT
Polymer 47 (2006) 5909–5918
polymer
www.elsevier.com/locate/polymer

Constructing polymer brushes on multiwalled carbon nanotubes by in situ reversible addition fragmentation chain transfer polymerization

Guoyong Xu [a], Wei-Tai Wu [a], Yusong Wang [a], Wenmin Pang [a], Qingren Zhu [a,*], Pinghua Wang [b], Yezi You [b]

[a] *Hefei National Laboratory for Physical Sciences at the Microscale, Structure Research Laboratory, University of Science and Technology of China, Chinese Academy of Sciences, Hefei 230026, PR China*

[b] *Department of Polymer Science and Engineering, Hefei University of Technology, Hefei 230009, PR China*

Received 26 November 2005; received in revised form 5 June 2006; accepted 11 June 2006
Available online 7 July 2006

Abstract

A fascinating nanoobject, diblock polymer brushes with a hard core of multiwalled carbon nanotubes (MWNTs) and a relatively soft shell of poly(methylmethacrylate)-*block*-polystyrene (PMMA-*b*-PS), was easily constructed by in situ reversible addition fragmentation chain transfer polymerization (RAFT) of methylmethacrylate followed by styrene (St) on the modified convex surfaces of MWNTs (MWNT–PMMA). The structure and morphology of the hybrid nanomaterials were characterized by FTIR, TEM, SEM, NMR, DSC and TGA. The results showed that both styrene and acrylate type monomers can be easily initiated and then propagated on the MWNT sidewalls via the in situ RAFT approach, and the length of the PS blocks increases with increasing St:MWNT–PMMA weight feed ratio.

Keywords: Carbon nanotubes; RAFT polymerization; Nanocomposites

1. Introduction

The great interest in carbon nanotubes (CNTs) resides in their possible technological applications in various fields of science, such as molecular wires, molecular electronics, sensors, probes, high-strength fibers, field emission, biological electronics devices, and hydrogen storage [1–12]. But their insolubility in solvents due to strong intertube van der Waals attraction impedes their application [1]. Noncovalent or covalent functionalization has improved the solubility. Noncovalent functionalization methods include dispersion with low molar mass or block copolymer surfactants [13–15], polymer wrapping [14,16–20], and polymer absorption [21,22]. The advantage of noncovalent attachment is that the nanotube structure and its electronic properties are not altered, but the surfactants and polymers that can be used for this method are limited. Covalent functionalization has been realized by using esterification and amidation reactions through the ''grafting to'' method [2,23]. However, the loss in conformational entropy of the polymer significantly suppresses chain from diffusing to and reacting with the carboxylic acid sites of single or multiwalled carbon nanotubes (SWNTs or MWNTs), which leads to inefficient grafting.

A polymer brush is an assembly of polymer chains that are tethered by one end to a substrate [24,25], such as a silicon wafer [25–29], gold, latex, clay, carbon black particles [25,30–32], and longer polymer backbones [33]. Polymer brushes have recently attracted considerable attention because of their novel structures and properties [25,34]. Polymer brushes were first synthesized by physisorption of block copolymers onto a substrate, with one block adsorbing strongly to the substrate surface and the other block forming the brush layer [35]. However, thermal and solvolytic desorptions of the brush due to the weak noncovalent nature of the grafting and a limited choice of functional groups for block polymer synthesis are two major disadvantages to this strategy. Covalent

* Corresponding author. Tel.: +86 551 3602813; fax: +86 551 3602803.
E-mail address: zhuqr@ustc.edu.cn (Q. Zhu).

0032-3861/$ - see front matter © 2006 Elsevier Ltd. All rights reserved.
doi:10.1016/j.polymer.2006.06.027

attachment of polymer chains to the surface can be accomplished by either ''grafting to'' or ''grafting from'' techniques. ''Grafting to'' technique involves the bonding of a preformed end-functionalized polymer to reactive surface groups on the substrate [36]. The limitation in this technique is that the attachment of a small number of chains hinders diffusion of additional macromolecules to the surface, thereby leading to low grafting density. The ''grafting from'' technique involves immobilization of initiators onto the substrate followed by in situ surface-initiated polymerization to generate the tethered polymer chains [25]. The advantage of this technique is that polymer brushes with high grafting density are easily synthesized. For better control of molecular weight and molecular weight distribution of the tethered polymers and to form block copolymer brushes, living radical, anionic, carbocationic and ring-opening metathesis polymerizations have been used in ''grafting from'' methods [25,27,29,30,37,38]. Some polymer chains also have been successfully grafted onto the surfaces of carbon nanotubes via this method, and they improved the properties of carbon nanotubes greatly [39,40–44]. Living radical polymerization, especially reversible addition fragmentation chain transfer polymerization (RAFT) [45] is the method used most to graft polymer chains of controlled molecular weight and molecular weight distribution from silicon wafers, gold particles, and polymer backbones.

Here we report on an application of the ''grafting from'' strategy to functionalize carbon nanotubes with RAFT method. Given the merits of living/reversible addition fragmentation chain transfer polymerization (RAFT), a very powerful tool for building of polymeric materials, we recently advanced the grafting-from approach, and realized in situ polymerization of styrene-type and acrylamide-type monomers on the surfaces of MWNTs [46]. Obviously, the method will significantly extend the optional monomers and then facilitate the fabrication of more novel CNT-based nanomaterials at relatively low cost. Moreover, this approach also provides an easy way to functionalize MWNTs further to synthesize polyblock or other complex structures. Block copolymer brushes are interesting due to the fact that vertical phase separation results when the block copolymer chains are tethered by one end to a surface or substrate. By changing the grafting density, chain length, relative block length, composition of the blocks or the interaction energy between the blocks and the surrounding environment, the formation of a variety of novel well-ordered structures has been predicted by theory [47] and in some cases demonstrated experimentally [48].

2. Experimental

2.1. Materials

The MWNTs used were purchased from Tsinghua-Nafine Nano-Power Commercialization Engineering Centre in Beijing. Bromoisobutyric acid (98%) was purchased from Aldrich. Styrene and methylmethacrylate (MMA) were obtained from Shanghai Reagents Co. The inhibitor was removed by passage through an alumina column and vacuum distillation. 2,2′-Azobis(isobutyronitrile)(AIBN) was purified by recrystallization from ethanol. Thionyl chloride ($SOCl_2$), tetrahydrofuran (THF), *N*,*N*-dimethylformamide (DMF), methanol, ethanol, chloroform ($CHCl_3$), glycol ($HOCH_2CH_2OH$), and other organic reagents or solvents were obtained from domestic market.

2.2. Synthesis of 2-hydroxylethyl-2′-bromoisobutyrate ($HOCH_2CH_2OCOC(CH_3)_2Br$, HEBrIB)

HEBrIB was synthesized by the following steps: 42.0 g (0.67 mol) of ethylene glycol, 11.2 g (0.067 mol) of 2-bromoisobutyric acid, 0.2 g (9.0×10^{-4} mol) of *p*-toluenesulfonic acid, and 100 mL of benzene were added into a 250 mL one-necked round bottom flask equipped with a magnetic stirrer. The mixture was heated at 96 °C while stirring for 36 h, and the water generated by the esterification reaction was removed through an oil–water separator. Then the reaction mixture was poured into 500 mL of distilled water and the lower, light-yellow, organic phase was separated. The organic portion was dissolved in methylene chloride and dried over anhydrous magnesium sulfate overnight. After filtration from the magnesium salt, and removal of solvent, 2-hydroxylethyl-2′-bromoisobutyrate was obtained as a colorless liquid (9.7 g, 68%). ^{1}H NMR (400 MHz, $CDCl_3$): δ 1.9 (s, 6H, 2-CH_3), 3.7 (t, 2H, OCH_2CH_2OH), 4.30 (t, 2H, $-COOCH_2CH_2-$).

2.3. Synthesis of MWNT–Br

In a typical experiment, crude MWNTs (3.0 g) were treated with a 60% HNO_3 aqueous solution (40 mL) in an ultrasonic bath (40 kHz) for 20 min and stirred for 24 h at reflux. Then the mixture was vacuum-filtered through 0.22 μm poly(tetrafluoroethylene) (PTFE) membrane and washed with distilled water until the pH of the filtrate reached 7.0. The filtered solid was dried under vacuum for 24 h at 50 °C, obtaining MWNT–COOH (2.2 g).

The carboxylic acids were converted into acyl chlorides by refluxing the as-prepared MWNT–COOH (2.0 g) with $SOCl_2$ (60 mL) in benzene (15 mL) at 70 °C for 24 h. Then the solvent was removed under vacuum. The remaining solid (MWNT–COCl) was washed three times with anhydrous THF and was dried under vacuum at room temperature for 5 h. A mixture of the solid (MWNT–COCl) (1.8 g), 2-hydroxylethyl-2′-bromoisobutyrate (10 mL), and 100 mL of anhydrous toluene was added into a flask and refluxed at 120 °C for 48 h. Then the solid was filtrated through a 0.22 μm PTFE membrane, thoroughly washed with ethanol and diethyl ether, and vacuum-dried for 24 h, affording 1.5 g of MWNT–Br.

2.4. Synthesis of MWNT–SC(S)Ph

Phenylmagnesium bromide (PhMgBr) was prepared from bromobenzene (25.0 g) and magnesium turnings (3.6 g) in anhydrous THF (150 mL). The solution was heated up to 50 °C and carbon disulfide was added over 15 min, then the reaction mixture was kept at 50 °C for 1 h. The MWNT–Br (1.1 g) was

added into the resultant brown mixture and the reaction temperature was kept at 60 °C for 72 h. Hydrochloric acid (1.0 M) was added and the product was washed with distilled water several times, then washed with ether several times. The RAFT agent functionalized MWNT (MWNT–SC(S)Ph) (0.92 g) was obtained by drying overnight under vacuum at room temperature.

2.5. Synthesis of MWNT–PMMA

MWNT–SC(S)Ph (40 mg), MMA (80 mg), and 0.1 mg of AIBN in 1 mL THF were added into a 5 mL polymerization tube. The polymerization tube was sealed under vacuum and placed in an oil bath at 90 °C and the contents were stirred for 48 h. At the end of the reaction the viscosity had increased dramatically. The mixture was subsequently diluted with $CHCl_3$ and vacuum-filtered with 0.22 μm PTFE membrane for three times. To ensure that no possible un-grafted polymer and free reagents were mixed in the product, the filtered mass was dispersed in $CHCl_3$, then filtered and washed with $CHCl_3$. The resulting solid was redispersed in 10 mL $CHCl_3$ and precipitated by the addition of 100 mL of methanol. The PMMA-coated MWNT sample (MWNT–PMMA) (65 mg) was obtained by filtering and drying overnight under vacuum. The parallel experiment, in which MWNT–SC(S)Ph was mixed with free PMMA in THF solvent followed by efficient filtration and washing, proved that the adsorbed PMMA quantity was lower than 3 wt%. Furthermore, NMR measurement for the upper layer of $CDCl_3$ solution, collected by centrifuging (2 h at a rate of 5000 rpm) MWNT–PMMA dispersed in the $CDCl_3$, showed that no PMMA signals appeared in the spectrum. This further indicated that the adsorbed polymer quantity was negligible.

2.6. Synthesis of MWNT–PMMA-b-PS

Typically, 20 mg of MWNT–PMMA, 80 mg of St and 0.1 mg of AIBN in 1 mL DMF were added into a 5 mL polymerization tube. The polymerization tube was sealed under vacuum and placed in an oil bath at 90 °C and the contents were stirred for 24 h. At the end of the reaction the viscosity had increased dramatically. The mixture was then diluted with $CHCl_3$ and vacuum-filtered with 0.22 μm PTFE membrane for three times. To ensure that no possible un-grafted polymer and free reagents were mixed in the product, the filtered mass was dispersed in $CHCl_3$, then filtered and washed with $CHCl_3$. The resulting solid was redispersed in 10 mL $CHCl_3$ and precipitated by the addition of 100 mL of methanol. The MWNT–PMMA-*b*-PS (60 mg) was obtained by filtration and drying overnight under vacuum.

Variation of St:MWNT–PMMA (8/1 and 12/1) gave rise to two other samples with different PS contents.

2.7. Characterization

FTIR spectra were recorded on a Magna-IR750 Fourier transform infrared instrument using KBr pellet method. X-ray photoelectron spectroscopy (XPS) was carried out on a VG ESCALAB MK Π system with Mg Kα radiation. NMR (^{1}H NMR, ^{13}C NMR) spectra were recorded on a Bruker Avance AV 400 spectrometer with $CDCl_3$ as solvent. All ^{13}C NMR spectra were recorded proton decoupled. Transmission electron microscopy (TEM) analysis was performed on a Hitachi-800 microscope at 200 kV, and the samples for TEM measurements were prepared by placing one drop of sample on copper grids coated with carbon. Scanning electron microscopy (SEM) images were recorded on a JEOL JSM-6300F field-emission microscope, and the samples were loaded on a glass surface previously sputter-coated with a homogenous gold layer for charge dissipation during the SEM imaging. Thermal gravimetric analyses (TGA) were carried out on a Shimadzu TGA-50H instrument with a heat rate of 10 °C/min. Differential scanning calorimetry (DSC) was performed on a Perkin Elmer Pyris Diamond DSC with a temperature gradient of 10 °C/min. The photo of the samples placed in a solvent was taken with a digital camera (Sony, DSC-P8).

3. Results and discussion

The RAFT polymerization has proven to be a versatile method for controlled radical polymerization of a variety of monomers. The mechanism involves the chain transfer of active species such as the radicals from decomposition of the initiator and propagating polymer radicals to the RAFT agent, forming an unreactive adduct radical, followed by fast fragmentation to a polymeric RAFT agent and a new radical. The radical then continues polymerization. The equilibrium is established by subsequent chain transfer-fragmentation steps between the propagating radicals and polymeric RAFT agents and continues until all monomers are consumed, resulting in controlled growth of chains.

3.1. Immobilization of surface RAFT agent onto MWNTs

Dithiobenzoate is an excellent RAFT agent for living radical polymerization of (meth)acrylate and styrene monomers. We chose to functionalize the sidewalls of MWNTs with carboxylic groups, followed by immobilizing the RAFT agent on the MWNTs and PMMA-*b*-PS brushes growing from MWNTs via surface RAFT polymerization (Fig. 1). The produced RAFT agent functionalized MWNTs (MWNT–SC(S)Ph) dispersed into organic solvents such as tetrahydrofuran (THF), dimethylformamide (DMF), and chloroform well enough to observe very broad bands in ^{1}H NMR spectrum, but it flocculates as black fiber bundles suspended in clear solvent in less than 1 week. Fig. 2 was the FTIR spectrum of the MWNT–SC(S)Ph. In FTIR measurements, the amount of sample added to the KBr disk must be strictly controlled so that it is less than the amount required for normal FTIR detection because the black MWNTs would absorb all the infrared rays if the amount of MWNTs was too much. For the appearance of a clear C–H stretch at ca. 2920 cm^{-1} and the appearance of a C=O, C=S stretch at 1730 cm^{-1}, 1060 cm^{-1}, respectively, we conclude that the RAFT agents have been covalently bound to the surface

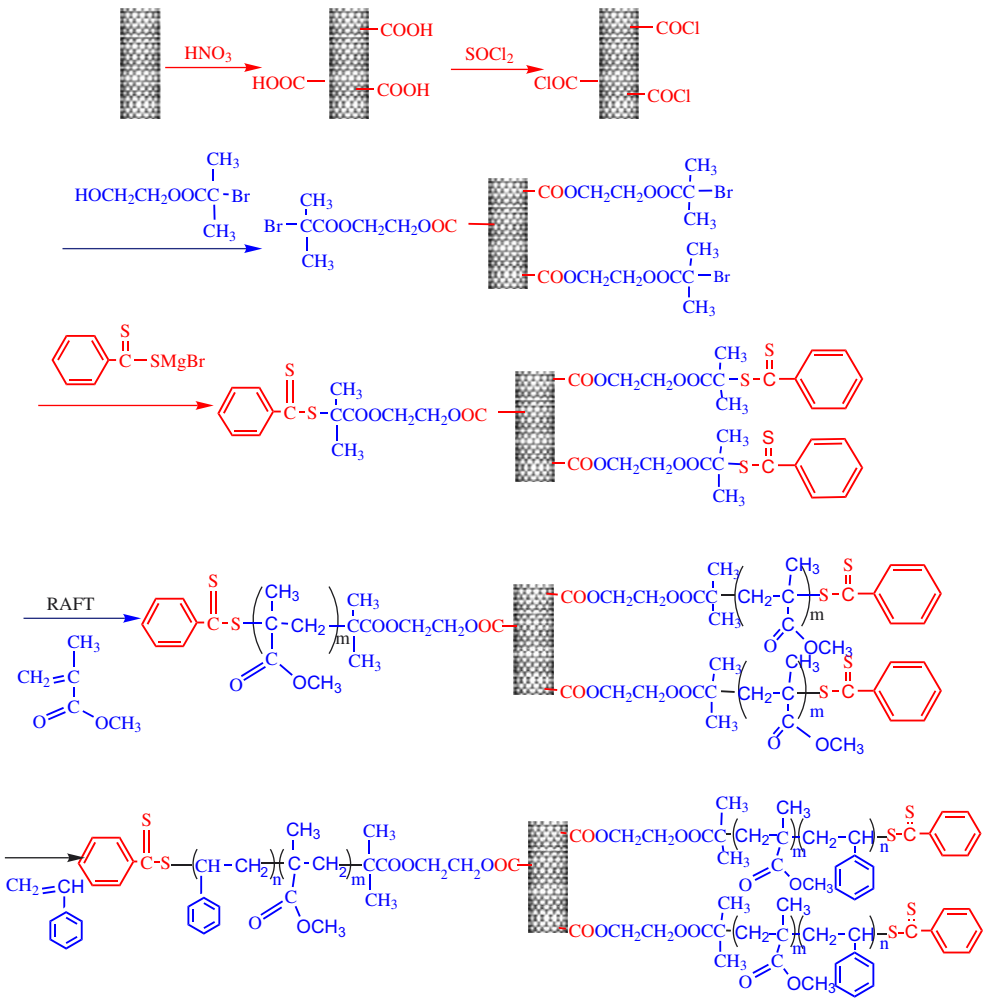

Fig. 1. Surface RAFT polymerization from MWNTs.

of MWNTs. TGA result showed about 0.78 RAFT agent functions per 100 carbon atoms calculated from the weight loss for MWNT–SC(S)Ph at 260–420 °C. In addition, X-ray photoelectron spectroscopy (XPS) analysis was employed to determine the composition of the MWNTs immobilized with RAFT agent. The result is shown in Fig. 3. The peaks at 284.60, 532.80 and 163.40 eV are attributed to C, O and S elements, respectively. The mole content of the RAFT agent on the surface of MWNTs is about 0.8% with respect to carbon, which is similar to the result obtained from TGA.

3.2. Solubility of the samples

In our experiments, the samples obtained in each step showed different solubility or dispersibility. The crude MWNTs were insoluble in polar and nonpolar solvents. After oxidation of MWNTs with HNO_3, polar carboxyl groups were introduced into the convex surface of MWNTs, so MWNT–COOH can be poorly dispersed in water and aggregated on the interface of chloroform and water. MWNT–SC(S)Ph exhibited very poor dispersibility in water but relatively good solubility in organic solvents. When the PMMA chains were attached to the surface of the nanotubes, the MWNT–PMMA showed a relatively good solubility in some solvents such as THF, $CHCl_3$, acetone, ether and toluene, almost similar to that of pure PMMA. MWNT–PMMA-*b*-PS displayed relatively good solubility in polar and nonpolar solvents such as THF, $CHCl_3$, toluene, DMSO and DMF.

Fig. 4 shows the digital photos of the samples of MWNTs (A), MWNT–SC(S)Ph (B), MWNT–PMMA (C), MWNT–PMMA-*b*-PS (4/1) (D) and MWNT–PMMA-*b*-PS (12/1) (E) placed in the incompatible solvent system ($H_2O/CHCl_3$) with different time. The pristine MWNTs were insoluble in H_2O and $CHCl_3$ solvents. The residual four samples are all soluble in $CHCl_3$ and insoluble in H_2O. The clear interface between H_2O and $CHCl_3$ solution can be observed after adding samples to the $H_2O/CHCl_3$ system. And we find that the polymer content of the samples influences the solubility in organic solvents. MWNT–SC(S)Ph flocculates as black fiber bundles suspended in clear solvent in less than 1 week. MWNT–PMMA-*b*-PS (4/1) containing 29.2% polymer is stable in $CHCl_3$ in less than 2 weeks. But MWNT–PMMA-*b*-PS (12/1), with 71.3% polymer fraction, showed good solubility in $CHCl_3$, forming a black solution which is stable for weeks. The deepening in color is attributable to the dissolved nanotubes, which possess extensively conjugated π electrons.

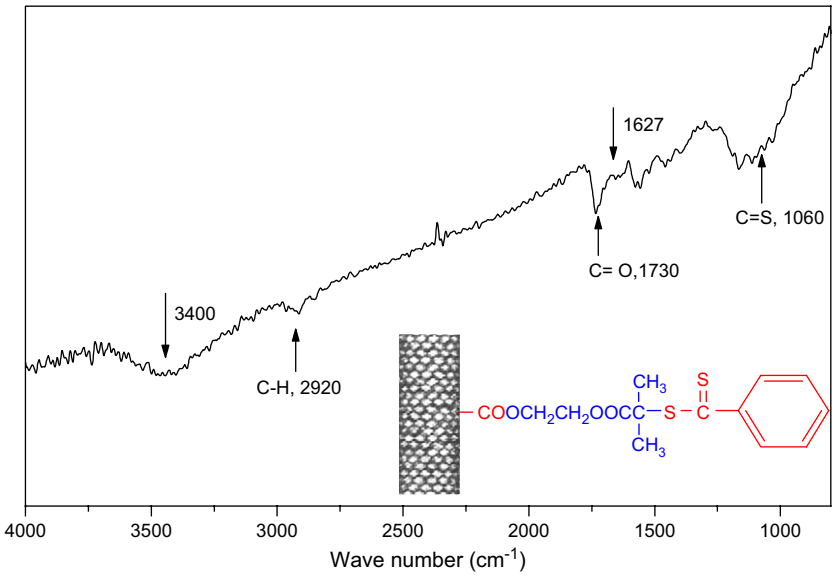

Fig. 2. FTIR spectrum of MWNT–SC(S)Ph.

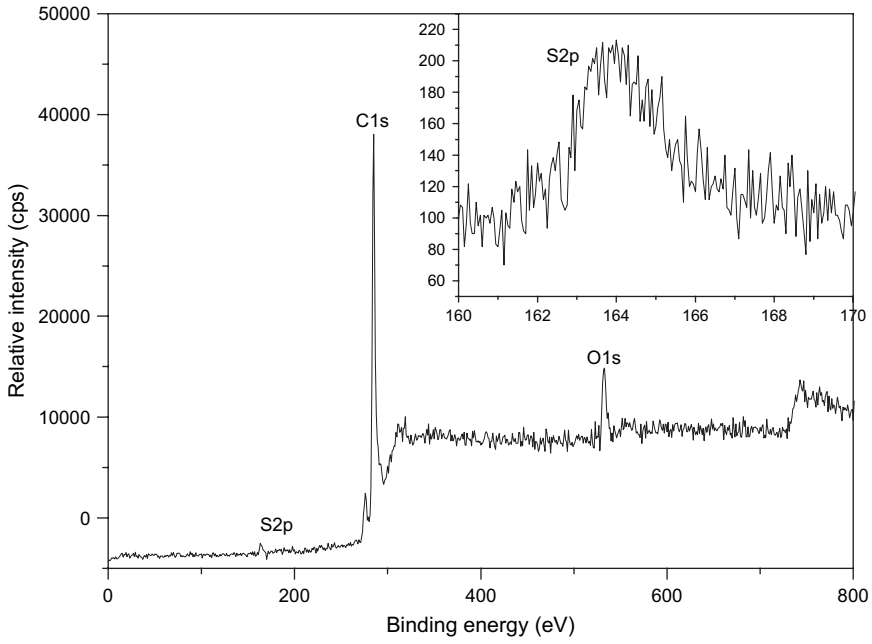

Fig. 3. XPS spectrum of MWNT–SC(S)Ph. Inset shows the corresponding high-resolution S2p spectrum.

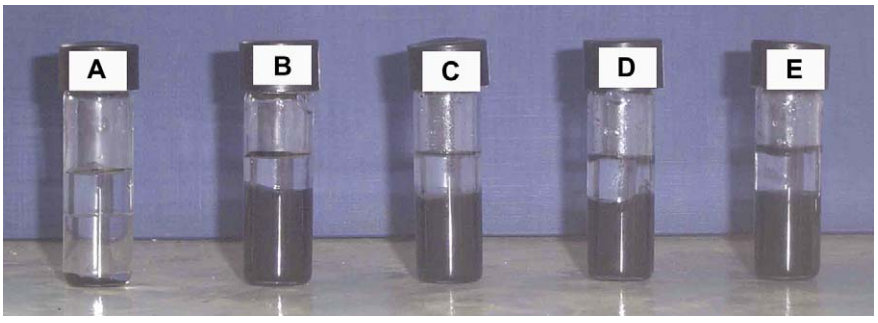

Fig. 4. The samples of MWNTs ($t = 0$) (A), MWNT–SC(S)Ph ($t = 2$ days) (B), MWNT–PMMA ($t = 1$ week) (C), MWNT–PMMA-*b*-PS (4/1) ($t = 1$ week) (D), and MWNT–PMMA-*b*-PS (12/1) ($t = 1$ month) (E) were placed in a mixed solvent of water (upper layer) and chloroform (bottom layer).

The different stability suggests that (1) the MWNTs are covalently bound grafted polymer and not adsorbed polymer, (2) such linkage strongly influences the physical properties of the tubes and (3) the density of copolymer modified nanotubes possibly has some contribution.

3.3. ^{1}H NMR, ^{13}C NMR and FTIR spectra

The chemical structure of the polymer moieties on the MWNTs was determined by ^{1}H NMR, ^{13}C NMR and FTIR spectra. In the ^{1}H NMR of MWNT–PMMA, the characteristic peaks of PMMA, such as the peak at $\delta = 3.6$ ppm ascribed to methyl proton of the ester unit and peak at $\delta = 1.0–2.8$ ascribed to the hydrogen species associated with the backbone of the grafted PMMA chain, were found (Fig. 5A). Notably, the peaks of the grafted PMMA did not broaden evidently as the previous literature reported [39a]. Considering that any free polymer can easily be removed by filtration, the NMR result is indicative of nanotube functionalization with the polymer. In the spectrum of MWNT–PMMA-*b*-PS, the phenyl-proton peaks of PS were observed at $\delta = 6.3–7.2$ ppm (Fig. 5B). The molar ratios of PS to PMMA units calculated from the integration areas of corresponding ^{1}H NMR spectra for three samples of MWNT–PMMA-*b*-PS were ~0.37/1, 2.1/1 and 3.0/1, respectively. Therefore, the chain length of PS building blocks coated on MWNTs can be controlled by the feed ratio.

Furthermore, the chemical structure of the polymer moieties on the MWNTs was determined by ^{13}C NMR. In the ^{13}C NMR of MWNT–PMMA, the characteristic carbon signals of PMMA, such as CH_3O-, CCH_2-, CCH_2- appeared at $\delta = 52.2$, 41.4 and 30.1 ppm, respectively (Fig. 6A). In the ^{13}C NMR spectrum of MWNT–PMMA-*b*-PS, the phenyl-carbon peaks of PS were observed at $\delta = 120–150$ ppm (Fig. 6B).

On the other hand, the characteristic absorption bands (e.g., $\nu_{C=C}$, $\nu_{C=O}$, ν_{C-H}, etc.) for the resulting samples were also found in their FTIR spectra (Fig. 7). For instance, a strong

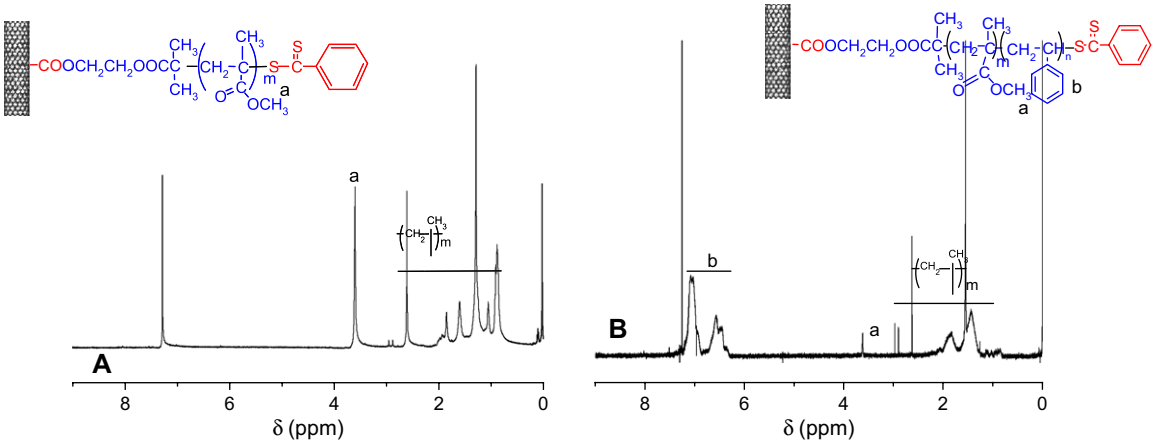

Fig. 5. ^{1}H NMR spectra of MWNT–PMMA (A) and MWNT–PMMA-*b*-PS (B).

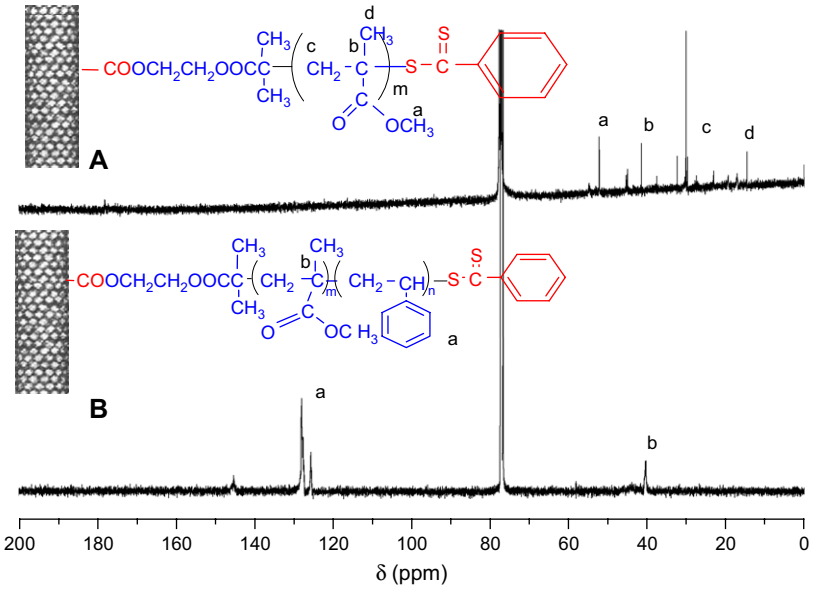

Fig. 6. ^{13}C NMR spectra of MWNT–PMMA (A) and MWNT–PMMA-*b*-PS (B).

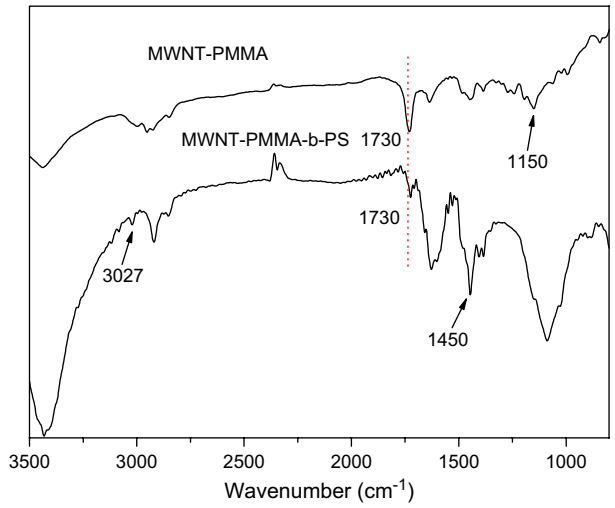

Fig. 7. FTIR spectra of the resulting samples.

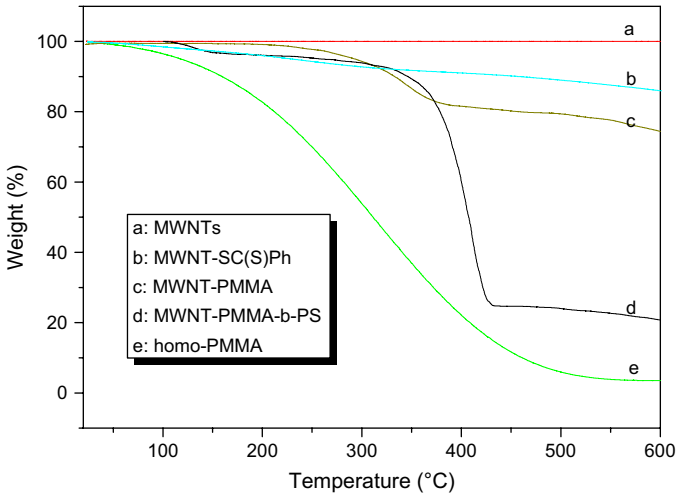

Fig. 8. TGA curves of the crude MWNTs, functionalized MWNTs and free PMMA.

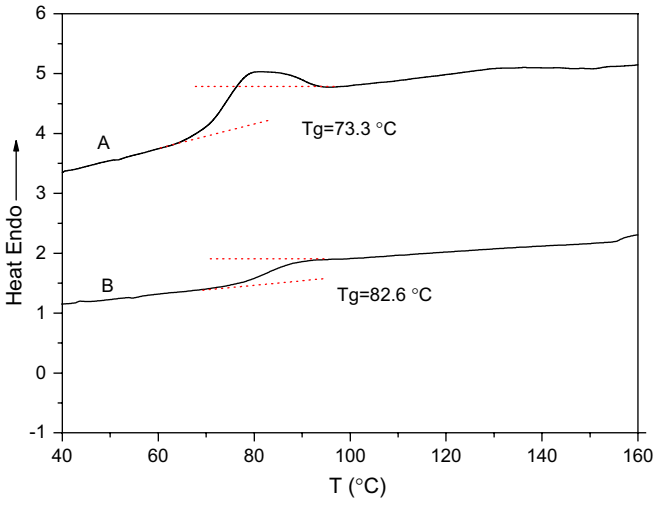

Fig. 9. DSC traces for MWNT–PMMA (A) and MWNT–PMMA-*b*-PS (8/1) (B).

C=O (ca. 1730 cm^{-1}) and C–O (ca. 1150 cm^{-1}) stretch, the characteristic peaks of PMMA, appeared in the spectrum of MWNT–PMMA. When the PS was polymerized to MWNT–PMMA, the peaks between 1450–1600 cm^{-1}, 1800–2000 cm^{-1}, and 3027 cm^{-1} of the characteristic absorption bands of PS were found. All these absorption data further suggested that the synthesis of MWNT–PMMA and MWNT–PMMA-*b*-PS was successful.

3.4. TGA and DSC analyses

TGA results give further evidence regarding the content and species of polymer layers grafted on MWNTs since the polymer and MWNTs parts have distinct thermal stabilities. As shown in Fig. 8, the sample of crude MWNTs is steady without significant weight loss below 600 °C. The sample of MWNT–SC(S)Ph displays weight loss of ~15% between

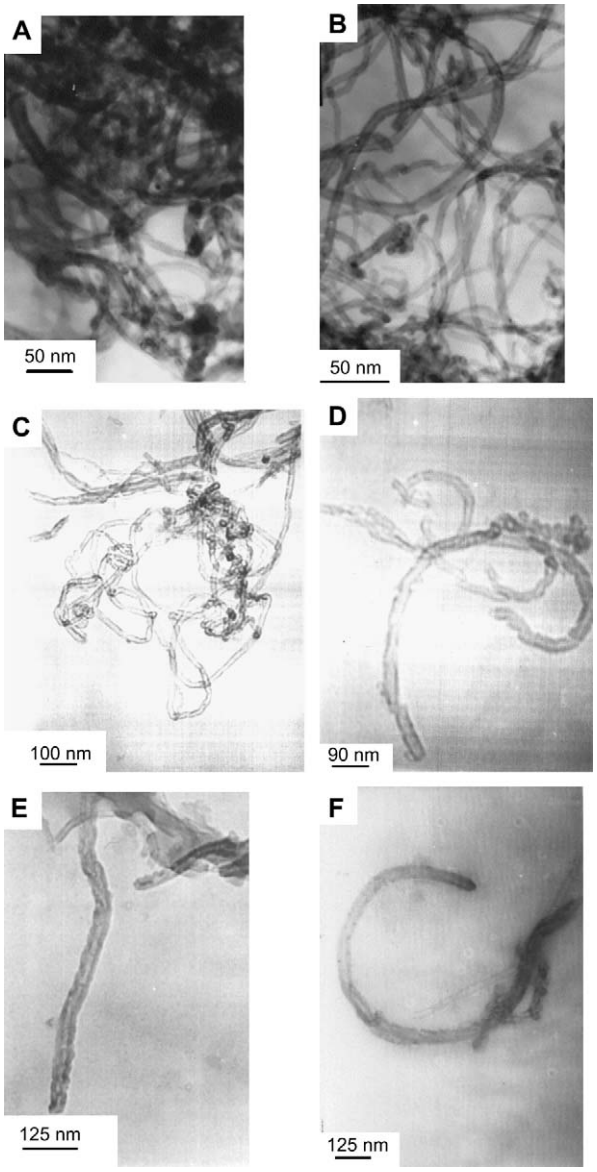

Fig. 10. TEM images of crude MWNTs (A), MWNT–SC(S)Ph (B), MWNT–PMMA (C, D) and MWNT–PMMA-*b*-PS (E, F).

100 and 600 °C. For the MWNT–PMMA sample, the onset of decomposition of PMMA moieties is ~300 °C, and the content of PMMA layers is ~20 wt%. For the MWNT–PMMA-*b*-PS sample, there are three main weight-loss regions. The first weight-loss region below ~200 °C can be assigned to the decomposition of free carboxyl groups on the surface of MWNTs. The rapid weight decrease in the second region (~200–420 °C, the onset is at ~300 °C) may readily be attributed to the decomposition of PMMA (~300 °C) and PS (~360 °C) polymers. The significant weight reduction in the third region (~420–600 °C, the onset is at ~500 °C) is likely due to the decomposition of MWNTs and the residual PS segments. The molar ratios of PS to PMMA units in three samples of MWNT–PMMA-*b*-PS calculated from the TGA data are ~0.35/1, 2.0/1, 3.2/1, respectively, which are in agreement with the results obtained from ^{1}H NMR spectra. Fig. 9 illustrates the differential scanning calorimetry traces for MWNT–PMMA (A) and MWNT–PMMA-*b*-PS (8/1) (B). T_g of the MWNT–PMMA is ~73.3 °C, while that of the commercial PMMA normally having a molecular weight of hundreds of thousand grams per mole is ~108 °C. The lower T_g suggests that the molecular weight of the PMMA grafts on MWNTs is not very high [49]. MWNT–PMMA-*b*-PS (8/1) shows only one T_g (~82.6 °C) (the value was between that of the MWNT–PMMA and PS (~100 °C) [50]). The microphase separation cannot be formed because the chain length of PMMA was too short [51]. It shows the blocks of PMMA and PS have a good miscibility in our sample.

3.5. TEM and SEM images of the crude MWNTs and the resulting functionalized MWNTs

The TEM images of the crude and functionalized MWNTs are shown in Fig. 10. The average internal and external diameters of the crude nanotubes are about 5–10 and 20–30 nm, respectively. The MWNTs wall consists of 10–25 graphite layers. The average length of the MWNTs is approximately several micrometers. In the image of crude MWNTs

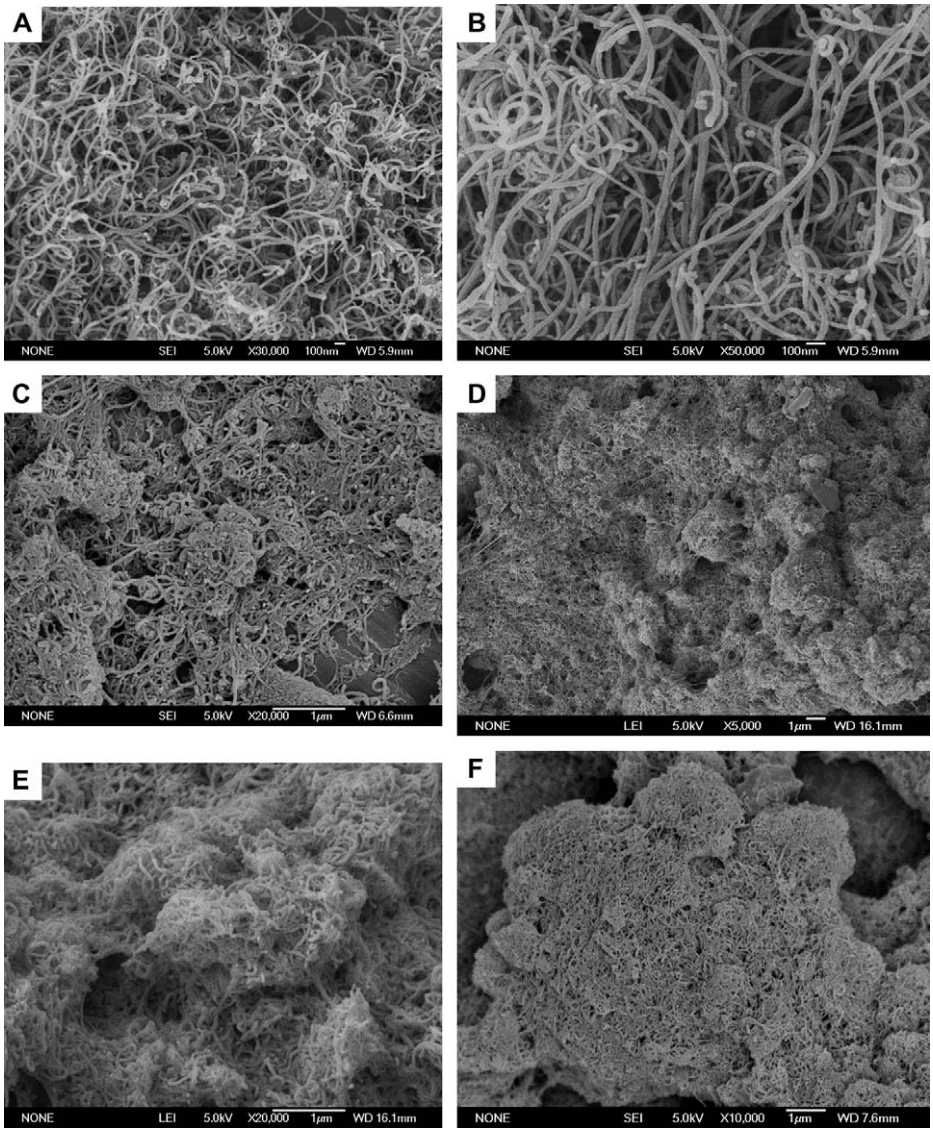

Fig. 11. SEM images of crude MWNTs (A, B), MWNT–PMMA (C, D) and MWNT–PMMA-*b*-PS (E, F).

(Fig. 10A), the diameters and the numbers of walls of MWNTs are not completely identical with one another and the jointed tubes mass together seriously. When the RAFT agent was attached to the surface of MWNTs, the carbon nanotubes dispersed well (Fig. 10B). So the MWNT–SC(S)Ph exhibited good solubility in weakly polar or nonpolar solvents such as THF, $CHCl_3$, toluene and hexane. For the samples of MWNT–PMMA, it can be found that some of the jointed tubes still mass together (Fig. 10C), but from the whole image, all the nanotubes were wrapped evenly with the polymer layers (Fig. 10D). Notably, the thickness of polymer layers grown on different sections of one tube is not the same because of the randomly scattered defects on MWNTs. In the copolymer functionalized MWNTs, the two polymer layers were even observed individually in the TEM image with different degrees of gray (Fig. 10E, F). Also no separate polymer phase was observed in the TEM image of the MWNT–PMMA and MWNT–PMMA-*b*-PS samples. Furthermore, because MWNT–PMMA-*b*-PS was made from the further polymerization of St on MWNT–PMMA, the thickness of its polymer layers was greater than that of MWNT–PMMA, which was clearly proved by the TEM images (Fig. 10). Fig. 11 displays the SEM images of the crude and functionalized MWNTs. As a comparison, SEM image of non-grafted tubes exhibits clearly distinctive tubelike morphology (Fig. 11A, B), while rodlike morphology was observed when the MWNTs were grafted with PMMA (Fig. 11C, D). The evidence for coated polymer brushes can be discerned from the reduced spacing between the nanotubes. When PS was polymerized on MWNT–PMMA, the rods become less distinct with eventually only a compact mass being observed (Fig. 11E, F).

4. Conclusions

Novel MWNT-based polymer brushes have been prepared via the RAFT agent immobilized on the surface of MWNTs. The related covalent functionalization has been confirmed by TEM, NMR and TGA characterizations. The attractive hybrid and its precursors exhibited different dispersibility in solvents. The results showed that the monomers can be easily initiated and then propagated on the MWNTs sidewalls, resulting in high density polymer-coated MWNTs, fascinating core–shell hard–soft nanoobjects. The advantageous grafting-from strategy is expected to open up an avenue for the functionalization of carbon nanotubes and the fabrication of novel carbon nanotube-based nanomaterials or nanodevices with designable structures and tailor-made properties. The polymerization with other monomers, kinetics of the polymerization and the solvent properties of the polymer-*g*-MWNTs are under investigation.

Acknowledgments

This work was supported by the National Science Foundation of China (No. 50573016), and the Open Foundation of Structural Research Laboratory of USTC.

References

[1] Baughman RH, Zakhidov AA, de Heer A. Science 2002;297:787.
[2] Chen J, Hamon MA, Hu H, Chen Y, Rao AM, Eklund PC, et al. Science 1998;282:95.
[3] Liu J, Rinzler AG, Dai HJ, Hafner JH, Bradley RK, Boul PJ, et al. Science 1998;280:1253.
[4] Keren K, Berman RS, Buchstab E, Sivan U, Braun E. Science 2003;302:1380.
[5] Balavoine F, Schultz P, Richard C, Mallouh V, Ebbesen TW, Moiskowski C. Angew Chem Int Ed 1999;38:1912.
[6] Williams KA, Veenhuizen PTM, de la Torre BG, Eritja R, Dekker C. Nature 2002;420:761.
[7] Dieckmann GR, Dalton AB, Johnson PA, Razal J, Chen J, Giordano GM, et al. J Am Chem Soc 2003;125:1770.
[8] Choi YK, Gotoh Y, Sugimoto K, Song SM, Yanagisawa T, Endo M. Polymer 2005;46:11489.
[9] (a) Pötschke P, Brünig H, Janke A, Fischer D, Jehnichen D. Polymer 2005;46:10355;
(b) McNally T, Pötschke P, Halley P, Murphy M, Martin D, Bell SEJ, et al. Polymer 2005;46:8222;
(c) Kim GM, Michler GH, Pötschke P. Polymer 2005;46:7346.
[10] Broza G, Kwiatkowska M, Roslaniec Z, Schulte K. Polymer 2005;46:5860.
[11] Zilli D, Chiliotte C, Escobar MM, Bekeris V, Rubiolo GR, Cukierman AL, et al. Polymer 2005;46:6090.
[12] Kashiwagi T, Du F, Winey KI, Groth KM, Shields JR, Bellayer SP, et al. Polymer 2005;46:471.
[13] Islam MF, Rojas E, Bergey DM, Johnson AT, Yodh AG. Nano Lett 2003;3:269.
[14] (a) O'Connell MJ, Bachilo SM, Huffman CB, Moore VC, Strano MS, Haroz EH, et al. Science 2002;297:593;
(b) O'Connell MJ, Boul P, Ericson LM, Huffman C, Wang Y, Haroz E, et al. Chem Phys Lett 2001;342:265.
[15] Kang Y, Taton TA. J Am Chem Soc 2003;125:5650.
[16] (a) Star A, Stoddart JF, Steuerman D, Diehl M, Boukai A, Wong EW, et al. Angew Chem Int Ed 2001;40:1721;
(b) Star A, Steuerman DW, Heath JR, Stoddart JF. Angew Chem Int Ed 2002;41:2508.
[17] Zeng H, Gao C, Wang Y, Watts PCP, Kong H, Cui X, et al. Polymer 2006;47:113.
[18] Brown JM, Anderson DP, Justice RS, Lafdi K, Belfor M, Strong KL, et al. Polymer 2005;46:10854.
[19] Ham HT, Choi YS, Jeong N, Chung IJ. Polymer 2005;46:6308.
[20] (a) Zhao C, Hu G, Justice R, Schaefer DW, Zhang S, Yang M, et al. Polymer 2005;46:5125;
(b) Hu G, Zhao C, Zhang S, Yang M, Wang Z. Polymer 2006;47:480.
[21] Gomez FJ, Chen RJ, Wang D, Waymouth RW, Dai H. Chem Commun 2003;3:190.
[22] Barraza HJ, Pompeo F, O'Rear EA, Resasco DE. Nano Lett 2002;2(8):797–802.
[23] Sun YP, Fu K, Lin Y, Huang W. Acc Chem Res 2002;35:1096.
[24] Milner ST. Science 1991;251:905.
[25] Zhao B, Brittain WJ. Prog Polym Sci 2000;25:677.
[26] Huang W, Skanth G, Baker GL, Bruening ML. Langmuir 2001;17:1731.
[27] Matyjaszewski K, Miller PJ, Shukla N, Immaraporn B, Gelman A, Luokala BB, et al. Macromolecules 1999;32:8716.
[28] Husseman M, Malmstroem EE, McNamara M, Mate M, Mecerreyes D, Benoit DG, et al. Macromolecules 1999;32:1424.
[29] Ejaz M, Yamamoto S, Ohno K, Tsujii Y, Fukuda T. Macromolecules 1998;31:5934.
[30] Ohno K, Koh KM, Tsujii Y, Fukuda T. Macromolecules 2002;35:8989.
[31] Vestal CR, Zhang ZJ. J Am Chem Soc 2002;124:14312.
[32] Liu T, Jia S, Kowalewski T, Matyjaszewski K, Casado-Portilla R, Belmont J. Langmuir 2003;19:6342.
[33] (a) Beers KL, Gaynor SG, Matyjaszewski K, Sheiko SS, Moeller M. Macromolecules 1998;31(26):9413–5;

(b) Boerner HG, Beers K, Matyjaszewski K, Sheiko SS, Moeller M. Macromolecules 2001;34:4375;
(c) Matyjaszewski K, Qin S, Boyce JR, Shirvanyants D, Sheiko SS. Macromolecules 2003;36:1843.
[34] Ito Y, Nishi S, Park YS, Imanishi Y. Macromolecules 1997;30:5856.
[35] Hadziioannou G, Patel S, Granick S, Tirrell M. J Am Chem Soc 1986; 108:2869.
[36] Mansky P, Liu Y, Huang E, Russell TP, Hawker C. Science 1997;275:1458.
[37] (a) Jordan R, Ulman A. J Am Chem Soc 1998;120(2):243–7;
(b) Jordan R, Ulman A, Kang JF, Rafailovich MH, Sokolov J. J Am Chem Soc 1999;121:1016.
[38] Weck M, Jackiw JJ, Rossi RR, Weiss PS, Grubbs RH. J Am Chem Soc 1999;121:4088.
[39] (a) Kong H, Gao C, Yan D. J Am Chem Soc 2004;126:412;
(b) Kong H, Luo P, Gao C, Yan D. Polymer 2005;46:2472.
[40] Kovtyukhova NI, Mallouk TE, Pan L, Dickey EC. J Am Chem Soc 2003; 125:9761.
[41] Georgakilas V, Kordatos K, Prato M, Guldi DM, Holzinger M, Hirsch A. J Am Chem Soc 2002;124:760.
[42] Khabashesku VN, Billups WE, Margrave JL. Acc Chem Res 2002;35: 1087.
[43] Bahr JL, Tour JM. J Mater Chem 2002;12:1952.
[44] Qin S, Qin D, Ford WT, Resasco DE, Herrera JE. J Am Chem Soc 2004; 126:170.
[45] Pyun J, Matyjaszewski K. Chem Mater 2001;13:3436.
[46] (a) Cui J, Wang WP, You YZ, Liu CH, Wang PH. Polymer 2004;45: 8717;
(b) Hong CY, You YZ, Pan CY. Chem Mater 2005;17:2247.
[47] (a) Zhulina EB, Singh C, Balazs AC. Macromolecules 1996;29:6338;
(b) Zhulina EB, Singh C, Balazs AC. Macromolecules 1996;29:8254.
[48] (a) Zhao B, Brittan WJ, Zhou W, Cheng SZD. Macromolecules 2000;33: 8821;
(b) Zhao B, Brittan WJ, Zhou W, Cheng SZD. J Am Chem Soc 2000;122: 2407;
(c) Boyes SG, Brittain WJ, Weng X, Cheng SZD. Macromolecules 2002; 35:4960.
[49] Cshich YT, Liu GL, Hwang KC, Chen CC. Polymer 2005;46: 10945.
[50] Li BC. Structures and physical properties of polymer. Beijing: Science Pub; 1989. p. 267.
[51] Ceresa RJ. Block and graft copolymerization. New York: Interscience Pub; 1973. p. 150.